Planetary and Space Science 70 (2012) 73–83

Contents lists available at SciVerse ScienceDirect

Planetary and Space Science

journal homepage: www.elsevier.com/locate/pss

Formulation of a wind specification for Titan late polar summer exploration

Ralph D. Lorenz [a,*], Claire E. Newman [b], Tetsuya Tokano [c], Jonathan L. Mitchell [d], Benjamin Charnay [e], Sebastien Lebonnois [e], Richard K. Achterberg [f]

[a] Space Department, Johns Hopkins University Applied Physics Laboratory, 11100 Johns Hopkins Road, Laurel, MD 20723, USA
[b] Ashima Research, 600 S. Lake Ave., Suite 303, Pasadena, CA 91106 and GPS, California Institute of Technology, 1200 E. California Blvd., Pasadena, CA 91125, USA
[c] Institut für Geophysik und Meteorologie, Universität zu Köln, Albertus-Magnus-Platz, 50923 Köln, Germany
[d] Earth & Space Sciences and Atmospheric & Oceanic Sciences, University of California, Los Angeles, 595 Charles Young Drive East, Los Angeles, CA 90095, USA
[e] Laboratoire de Meteorologie Dynamique, 4 Place Jussieu, Box 99, 75252 Paris, France
[f] Department of Astronomy, University of Maryland, College Park, MD 20742, USA

ARTICLE INFO

Article history:
Received 12 March 2012
Received in revised form
13 May 2012
Accepted 25 May 2012
Available online 6 June 2012

Keywords:
Titan
Winds
Atmospheric boundary layer
Spacecraft mission design

ABSTRACT

Titan's polar regions, and its hydrocarbon lakes in particular, are of interest for future exploration. The polar conditions have considerable seasonal variation and are distinct from the equatorial environment experienced by Huygens. Thus specific environmental models are required for these regions. This paper, informed by Cassini and groundbased observations and four independent Global Circulation Models (GCMs), summarizes northern summer polar conditions (specifically, regions north of 65°N, during the 2023–2024 period, or solar longitude $L_s \sim 150°$–$170°$) and presents a simple analytical formulation of expected, minimum and maximum winds as a function of altitude to aid spacecraft and instrument design for future exploration, with particular reference to the descent dispersions of the Titan Mare Explorer (TiME) mission concept presently under development. We also consider winds on the surface, noting that these (of relevance for impact conditions, for waves, and for wind-driven drift of a floating capsule) are weaker than those in the lowest cell in most GCMs: some previously-reported estimates of 'surface' wind speeds (actually at 90–500 m altitude) should be reduced by 20–35% to refer to the standard 10 m 'anemometer height' applicable for surface phenomena. A Weibull distribution with scale speed $C=0.4$ m/s and shape parameter $k=2.0$ embraces the GCM-predicted surface wind speeds.

1. Introduction

In contrast to the well-understood space vacuum environment, planetary atmosphere and surface environments are fraught with unknowns that are disconcerting to engineers charged with developing systems and instruments with constrained budgets that must have a specified probability of successful function. The best scientific information available must be applied in order to make quantitative estimates of the probability of encountering various conditions.

While the Huygens probe was designed with relatively few observational constraints on the environment to which it was sent and many engineering models simply had to be constructed from basic physical principles, the results from the Huygens descent, from improved groundbased observations and not least some 7 years of measurements by the Cassini orbiter give a much more informed perspective (e.g., Brown et al., 2009) on which to base designs for future Titan missions. Many unknowns have been resolved completely (e.g., Argon, feared to be present at levels which could affect radiative heat loading on probe entry shields, has now been determined to have a comfortably low abundance) and other issues such as topography, while incompletely known, at least now have enough data on which to base rational models.

Perhaps the most remarkable aspect of Titan revealed by the Cassini–Huygens mission (e.g., Lorenz and Mitton, 2008; Coustenis and Taylor, 2008; Brown et al., 2009) is its geographical diversity and in particular that there are major and systematic variations with latitude of the character of the surface and in properties of the atmosphere. Because of Titan's effective obliquity (actually, largely due to Saturn's obliquity of 26.7°: the inclination of Titan's orbit with respect to the Saturn ring plane, and in turn the obliquity of Titan with respect to its Saturnocentric orbit, are each less than half a degree and are climatologically negligible), the polar regions see considerable seasonal variation. Thus models developed for the Huygens mission – for the less seasonally-variable equatorial region – are not all applicable without modification.

This paper is an attempt to assess the Titan north summer polar environment (specifically, regions north of 65°N, during the

* Corresponding author. Tel.: +1 443 778 2903; fax: +1 443 778 8939
E-mail address: Ralph.Lorenz@jhuapl.edu (R.D. Lorenz).

0032-0633/$ - see front matter © 2012 Elsevier Ltd. All rights reserved.
http://dx.doi.org/10.1016/j.pss.2012.05.015

2023–2024 period, or solar longitude $L_s \sim 150^o$–170°) to permit credible design of missions and instruments for that location and season. This is of particular relevance given that the upcoming NASA Discovery-12 mission solicitation could permit Titan missions launching in 2015–2017 and thus arriving 2021–2024, towards the end of Northern Summer. The proximity of Earth and the sun (Earth is always within 6° of the sun as seen from Titan) mean that continuous or near-continuous direct-to-Earth communications are possible from the Titan surface under these conditions, making a mission feasible without an orbiter relay. The polar regions (and the north polar regions especially) are of interest because of the large number of hydrocarbon lakes (Stofan et al., 2007) and the three seas (Punga, Ligeia and Kraken Mare, in order of increasing size).

We first review the philosophy of engineering wind model development, and the approaches that have been adopted in Mars and Titan exploration. We then describe a proposed model specification for Ligeia in 2023–2024 and go on to compare with available model and observational data.

2. Wind modeling for planetary missions

Defining planetary environments presents the scientist with an interesting challenge. In general, there are only limited data upon which to base any definition, since after all the usual purpose of the mission in question is to measure the environment because so little is known. A definition should be simple in description, and must generally provide an envelope of possibilities that are unlikely to be exceeded (sometimes at the 99.5% or '3-sigma' level, although 99% and 95% or '2-sigma' are also used). To be assured of not encountering extremes beyond these bounds, the scientist should define a wide range. However, the larger the range that the system in question must perform in, the more difficult is the task for engineers confronted with designing it and the less affordable the mission becomes.

Thus the fundamental problem is to define a wind envelope that is as small as the available information (from models and observations) will allow. In principle, one can only be confident in a '99%' wind if one has hundreds of independent data points, such that the boundary can be defined by 1% of the points falling outside of it. Depending on the confidence in the data, one defensible approach is to simply define an envelope that spans all data points and add some margin. Here, and especially when very few data are available, some scientific judgment must be applied.

Often the assumption of a Gaussian distribution is used, in which case one third of the data should exceed one standard deviation (i.e., 'one sigma') and the required 99.5% envelope is simply three times larger. In actuality, wind speed distributions tend to be asymmetrical and have longer tails than Gaussian and so Weibull, Exponential or other distributions may be more appropriate. There may also be physical factors that should apply—e.g., a wind speed distribution with an expected value of 20 m/s and an 'uncertainty' (interpreted to be one-sigma) of 10 m/s, would have a 3-sigma lower limit of −10 m/s, yet a speed can only have a positive value. Similarly, one might find the range of specified winds exceeding some limit such as the speed of sound: one engineer's interpretation of the Flasar model led to an indication of physically-implausible supersonic winds, for example (Flasar, personal communication, 18th April 2012).

An even more fundamental assumption that is often adopted is that not only do values have a Gaussian distribution, but that they have a statistical basis at all. In reality, confidence intervals might be best seen as just that – a Bayesian measure of belief – rather than as an expectation that 0.5% of values will actually exceed the 'three sigma' value in the frequentist sense. Put another way, a wind is perhaps more likely to exceed a specification not because a random fluctuation has an improbable value, but rather because an assumption in the model was incorrect, a factor which cannot be readily quantified. This philosophical distinction, however, does not help the spacecraft designer. We will therefore proceed, recognizing the caveats above.

2.1. Mars missions

To date all the experience of landing at designated surface locations on other planetary bodies with atmospheres is from Mars missions. We thus first look to what has been done in this arena. For missions to the Martian surface, winds are in fact only a modest contributor to the dispersion of landing locations. This is for two main reasons. First, relatively shallow atmospheric entry is required at Mars to permit deceleration from orbital speeds without impacting the surface. This means that a modest uncertainty ellipse in the plane normal to the arrival direction becomes stretched by its shallow projection onto the sphere defining the entry interface. Thus the delivery uncertainty becomes quite large in the downrange direction, and any wind-driven descent dispersions are comparably small. Second, these descent dispersions are small in absolute terms because in the thin Martian atmosphere descent speeds, even with large parachutes, are high and thus descent is over in a matter of a few minutes. There is therefore no time for winds to displace a lander by a large distance.

However, winds are still important, principally in determining the horizontal component of spacecraft velocity at impact. While the vertical speed will usually be determined by the terminal velocity under the parachute, landing systems can usually only tolerate a modest sideways speed. Furthermore, certain modes of the spacecraft-parachute system – and in particular the 'scissors' mode where the spacecraft and parachute pivot in opposite directions, sometimes also referred to as the 'wrist' mode – can be excited by wind shear and there may be limits in the allowable angular rates of the vehicle.

Because only a very limited set of in-situ meteorology data exists, the principal basis on which the Entry Descent and Landing (EDL) risks of missions such as the Mars Exploration Rovers (e.g., Kass et al., 2003) and Phoenix (Tamppari et al., 2008) are defined is the output of numerical (and in particular site-specific mesoscale) models. Most recently for the Mars Science Laboratory MSL (now named Curiosity) wind considerations from mesoscale models were instrumental in rejecting some candidate landing sites. Model prediction of Mars winds has been rather successful since the thin atmosphere responds quickly to the deterministic solar forcing without the complications of oceans or moist convection.

2.2. Huygens

Although there was no requirement on the Huygens probe to survive operation post-landing, nor was there a specified landing site, it was recognized early in the formulation of the Huygens probe that winds could displace the vehicle horizontally by several hundred km from its entry point. This was important because the radio link relied on knowing the probe's position accurately to point Cassini's high gain antenna to receive the probe's data. The thick Titan atmosphere meant that descent would be some 2–3 h long, allowing time for winds to displace the vehicle by ~200–300 km. Furthermore, the dense atmosphere (and its large scale height) allows Titan atmospheric entry to be relatively steep, so the delivery uncertainty ellipse is not stretched into a large entry point uncertainty. Thus wind is the dominant contributor to the landing point uncertainty on Titan.

A wind model was formulated for mission design by Flasar of the NASA Goddard Space Flight Center in Phase A of the ESA Cassini Titan Atmosphere Probe study (prior to the mission being named 'Huygens'). This model (used for several years before its publication—Flasar et al., 1997) was an altitude profile of zonal wind speed based on the equator-to-pole gradient of thermal infrared brightness temperatures (initially simply brightness temperatures corrected for emission angle, later inversions of radiance were perfomed to derive temperatures along isobars). The model provided a minimum and maximum zonal wind as well as the 'nominal'. For most of the Huygens probe's development and flight, the possibility was allowed for that winds could be prograde or retrograde (in the cyclostrophic limit the thermal wind equation does not discriminate), although evidence steadily built for a prograde direction (as was expected all along). The first published prograde determination was by heterodyne spectroscopy of ethane emission (Kostiuk et al., 2001): a useful summary of this and subsequent observations is Kostiuk et al. (2006). The model assumed zero meridional and vertical winds, as well as zero winds at the surface.

Additional support for the estimated magnitude of the stratospheric zonal winds was given by the observation of oblateness in the Titan atmosphere, as indicated by the occultation of the star 28 Sag in 1989 (e.g., Hubbard et al., 1993). That data also suggested the possibility of high-speed jets at 60° latitude, although because it used a symmetric Fourier description could not discriminate between a jet in the winter hemisphere, the summer hemisphere, or both. Since that time GCMs, Cassini observations, and indeed the dual stellar occultation of 2003 (Sicardy et al., 2006), have shown that as on Earth, the jet is predominantly a winter polar phenomenon.

Despite the austere and indirect data from which it was derived, the Flasar wind model proved rather close to what was observed by Doppler tracking of the probe (Bird et al., 2005; Folkner et al., 2006). It slightly overpredicted winds in the troposphere (for which there was no data in any case), and the temperature field on which it was based lacked the resolution to suggest a shear layer which Huygens detected with near-zero winds at around 80 km altitude. Apart from that one excursion (which was high enough in the atmosphere not to be a major contributor to the net drift), the observed winds were between the extreme limits determined some 15 years earlier on the basis of only a handful of numerical values. It is also of note that a preliminary consideration of surface winds (suggested to be typically <0.6 m/s) by Allison (1992) appears broadly supported by the Huygens measurement and modern GCM results.

2.3. Models for early post-Cassini mission studies

A prominent NASA endeavor prior to Cassini was an agency-wide Aerocapture mission study, sponsored by the NASA In-Space Propulsion Program around 2003–2004. This study noted the utility of aerocapture for delivering vehicles to Titan orbit using atmospheric deceleration. To facilitate this work, and in particular the statistical variation of upper atmospheric density which is crucial to aerocapture performance, parametric variation of the available Huygens models (the Yelle density profile (Yelle et al., 1997), and the Flasar wind model) was encapsulated in the Titan-GRAM-2004 software package (Global Reference Atmosphere Model, Justus et al., 2004) Unfortunately, rather little attention was paid in this pre-Cassini effort to the accuracy of the wind parameterization which is not physical and was not subjected to peer review. Notably, the zonal winds for all latitudes are described roughly as the Flasar equatorial profile, without reduction at high latitude which is required to avoid infinite shear at the pole. Similarly, the dispersion on meridional winds is assumed to follow the same profile as that on zonal winds, which is comparable with the absolute value of the nominal wind profile. Such a model, with implied meridional winds of tens of meters per second, is clearly unphysical and grossly overpredicts dispersions on descent trajectories. Perhaps because winds have a minimal influence at aerocapture altitudes, these demonstrably incorrect specifications were not challenged at the time.

The first decade of the 21st century saw consideration of lighter-than-air platforms as possible post-Cassini exploration systems. An apparent limitation, given the assumed purely-zonal circulation, was that a vehicle without propellers (i.e., essentially acting as a Lagrangian tracer particle) would be confined to a single line of latitude. One approach to traverse north-south was a 'Stratosail' (Pankine et al., 2004), a wing suspended from a balloon to exploit the vertical gradient in zonal wind to develop a side-force to provide meridional motion: this study used the Flasar model, together with parameterized tidal winds (Tokano and Neubauer, 2002). A first effort to apply GCM results to Titan exploration mission studies was by Tokano and Lorenz (2006), who assumed a balloon in Titan's atmosphere floating at a constant altitude (2 km or 20 km) moving with the wind. An interesting result was that the latitudinal drift could be quite significant, if the balloon floated at an altitude wherein the zonal wind speed was resonant with the atmospheric tide—in effect the balloon could 'surf' a tidal wave.

2.4. Post-Cassini

The perspective for defining the wind-environment for future Titan missions is now much better-informed. Although Cassini data so far offer relatively few wind measurements, largely since there are few clouds to track and Cassini lacks instrumentation to directly measure stratospheric winds, the present understanding of Titan's meteorology is now considerably improved over that during the development of Huygens. In particular, Doppler tracking of the Huygens probe (Bird et al., 2005; Folkner et al., 2006) as well as optical odometry from descent images (Tomasko et al., 2005; Karkoschka et al., 2007) provides vital ground truth with which the ever-improving arsenal of models can be tuned. Some additional constraints on near-equatorial winds from ground-based observations (stellar occultations, as well as Doppler resolved near-IR and heterodyne thermal infrared spectroscopy) are summarized in Witasse et al. (2006). Additionally, while only a brief snapshot mapping of thermal emission from Voyager formed the basis for the successful wind model prediction by Flasar, there is now a very large database of coverage from Cassini over all latitudes over some 7 years that allows not only the wind field to be estimated, but part of its seasonal variation observed.

With this perspective, we can no longer talk about a 'Titan Wind Profile', but rather must refer to an environment at a specific latitude and season. A couple of general points may be noted. First, that polar zonal winds are in general rather weaker than those at lower latitudes, and broadly speaking may vary as the cosine of latitude in a 'solid body' rotation paradigm. (Note that the 'constant angular momentum' paradigm that may approximately hold near the equator – see e.g., Flasar et al. 1997; Porco et al., 2005 – cannot persist to the poles, where it would predict infinite wind speeds.) This general principle of winds declining at high latitude appears to be borne out in Global Circulation Models, which predict very modest stratospheric winds near the pole during most of the year. An exception to this is during polar winter, when a circumpolar stratospheric jet develops—as is the case on Earth and Mars. The fact that this phenomenon is common to several planetary bodies lends some confidence to these model predictions. During summer, however, stratospheric winds in both GCMs and in Cassini data (Achterberg

et al., 2011) seem to be relatively constant with time, and monotonic with latitude.

The other point is that although we recognize there may be some asymmetry between seasons due to the eccentricity of Titan's path around the sun, we can assume that northern summer winds (for which there are as yet no direct observations) are not substantially different from – or at least are no stronger than – southern summer winds, for which there is a useful body of data from groundbased observations starting around 2000 and from Cassini observations from its arrival in 2004. This assumption of symmetry is somewhat conservative for the season and hemisphere of interest for the present paper in that the solar flux in northern summer is 20% weaker than that in the southern summer. The assumption is also essential assumption in order to allow the present observation dataset to be applied to the model.

3. TiME zonal wind model specification

The principal flow throughout most of Titan's atmosphere is the prograde zonal circulation. Although this circulation can reverse at low altitudes, prograde motion dominates. As with the low-latitude winds that determined the Huygens drift, the zonal wind is the main factor in determining the landing (or splashdown) point of a near-polar parachute descent. In this section we first present our zonal wind model specification as analytic functions of altitude, and then using this as a common reference, introduce the various observational and model data that support this specification.

We will specify the 'nominal' wind profile, our best estimate of what a vehicle may encounter, on the basis of the observational data, namely Cassini cloud tracking and thermal wind measurements at the relevant latitude. We select the profiles that define the 99% maximum and minimum limits to exceed all model results. A variety of analytic forms could be chosen—in fact not unreasonable agreement with data can be obtained with a simple linear function of altitude. However, a description that fits the data best appears to be one that increases steeply with altitude in the troposphere and remains more or less constant above.

One such function is $U(z)=U_{300}/(1.0+\exp((z_o-z)/L)$ where U_{300} is the asymptotic stratospheric zonal wind speed at 300 km altitude, z is the altitude in km, L is a length scale and z_o a reference altitude. The relevant parameters are listed in Table 1. It should be noted that this succinct expression should not be used to assess winds at any other season or latitude, nor should it be applied to heights immediately above the surface (i.e., $z<2$ km, in the planetary boundary layer). We will consider those separately in a later section of the paper.

The resultant wind profiles are shown in Fig. 1, validated against various GCM and observational datasets described in the next section. Some representative values are listed in Table 2.

3.1. Zonal wind data

3.1.1. Thermal winds in the stratosphere

As discussed in "Wind modeling for planetary missions" section, the only information available at first to define the Huygens wind model was the equator-pole variation in thermal infrared brightness temperature from Voyager and the inferred thermal gradient winds. More extensive data of a similar type from the Cassini Composite Infrared Spectrometer (CIRS) are available to constrain stratospheric temperatures in late southern summer, and via the thermal wind equation, the zonal wind field (Flasar et al., 2005; Achterberg et al., 2011). Here, data from 2004 to 2009 for the latitude ~75°–80°S as shown in Achterberg et al. (2011) has been extracted and is plotted in Fig. 1a. Specifically, wind speeds of ~10 m/s at an altitude of ~100 km, and 20–25 m/s at ~200 km are indicated. These speeds are notably smaller – by about a factor of 3 – than those recovered from the same dataset at lower latitudes. As noted in "Post-Cassini" section, these late southern polar summer winds in 2004–2009 are assumed to be representative of late northern polar summer winds in the early 2020s.

Table 1
Parameters for zonal wind specification for 80° latitude, $L_s=160°$ following the equation $U(z)=U_{300}/(1.0+\exp((z_o-z)/L)$.

	U_{300} (m/s)	z_o (km)	L (km)
Nominal	22	35	8
Maximum	50	38	11
Minimum	−3	0	1

3.1.2. Cassini cloud tracking

A persistent frustration of Titan for meteorologists is the paucity of clouds that can be tracked to estimate winds. However, for the polar summer at least, a useful dataset exists, and is very important since the available thermal winds do not probe the troposphere. As reviewed by Flasar et al. (2010), tracking of 9 south polar summer clouds between 60° and 80°S by the Cassini ISS instrument in 2004 (Porco et al., 2005; Turtle et al., 2009; see also figure S3 of Turtle et al. (2011)) yielded estimates of zonal wind speed between 0 m/s and 3 m/s with a single feature at 16 m/s. This latter feature was also observed (with an estimated motion of the opacity center in near-IR data from the Cassini Visual and Infrared Mapping Spectrometer (VIMS) by Griffith et al. (2005). Bouchez and Brown (2005) determine 3σ upper limits on zonal motion of 4 m/s eastward and 2 m/s westward on clouds observed with Hale telescope at the Palomar observatory over 16 nights 2001–2003 at 72°–83°S. Other cloud-tracking measurements from groundbased data were reported by Schaller et al. (2006) and Hirtzig et al. (2006) and Cassini VIMS tracked clouds in summer 2004 (Brown et al., 2006).

These results are assembled in Fig. 2. The evident preponderance of the data indicate weak (~2 m/s) prograde winds. The ~16 m/s detection is a clear outlier—it could indicate a long tail in the wind distribution, but then the lack of detections between 7 m/s and 13 m/s is puzzling. One possibility is that the faster winds represent a different population of clouds, perhaps some that have ascended to the top of the troposphere where winds are stronger. The altitude inferred from spectral data in Griffith et al. (2005) suggests the cloud is at 40–45 km.

Thus our preferred interpretation of the aggregate of the cloud data is that most ($N=14$) are associated with the lower troposphere (10–20 km), and their speeds are approximately normally-distributed with a mean of 2 m/s and a standard deviation of 2 m/s, which allows for the single ~5.8 m/s detection. We will consider the faster cloud ($N=1$) as a separate detection at 40–45 km. These are the values plotted in Fig. 1i.

3.1.3. Huygens Doppler wind profile

Although the Huygens wind profile (Bird et al., 2005; Folkner et al., 2006) is not directly applicable to the polar summer, since it was obtained at both a different location and season (10°S, $L_s\sim300°$), it seems worthwhile to at least take it into account since as the only available in-situ measurement it represents our single best wind profile determination for Titan. Noting that the thermal wind data above indicates a factor of ~3 between low and high latitudes, we multiply the Huygens zonal wind profile as archived on the Planetary Data System multiplied by 0.3 to compare with our proposed model in Fig. 1b and Fig. 1g.

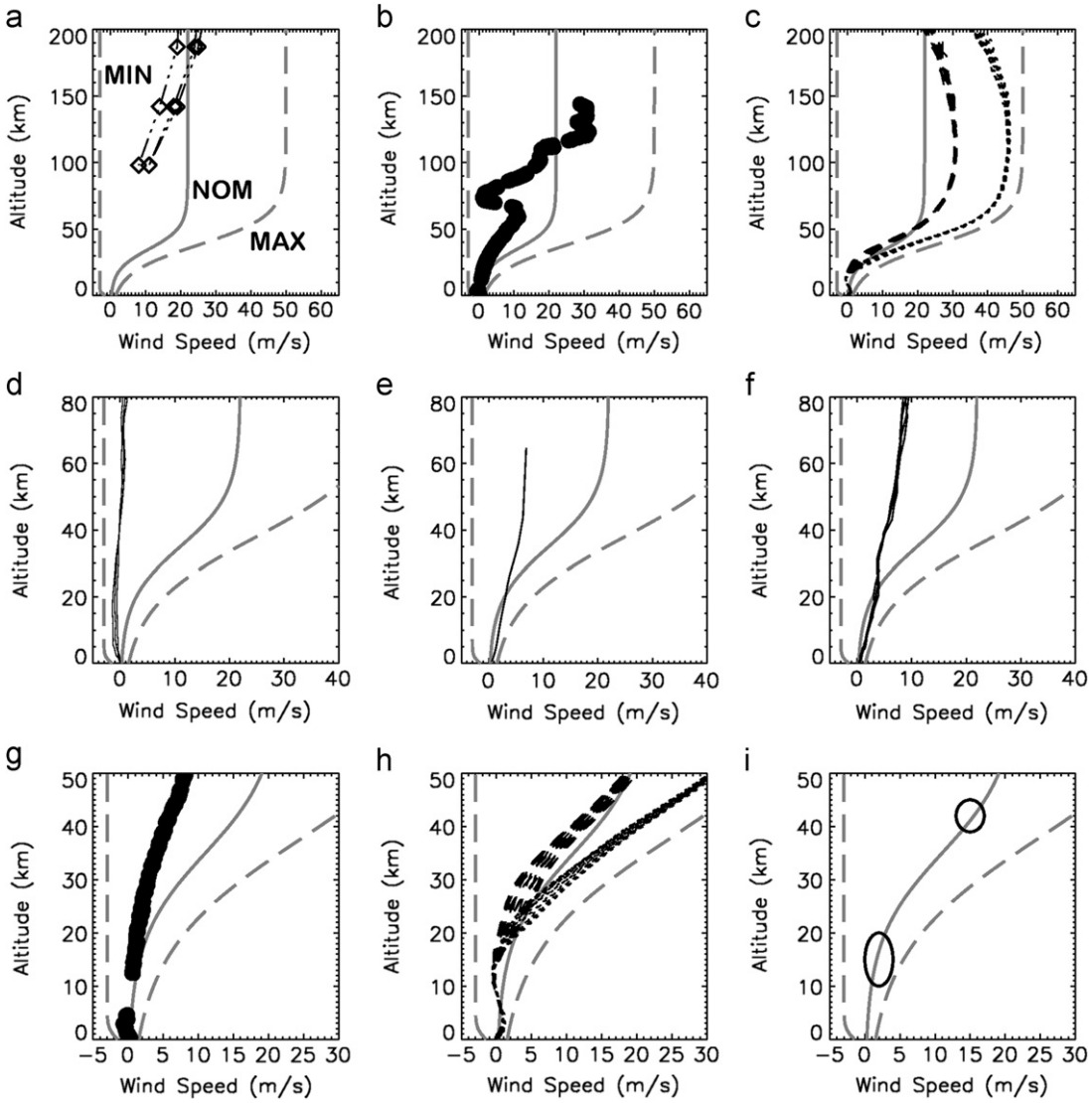

Fig. 1. Zonal wind model (solid gray curve for nominal profile; long-dashed curves for minimum and maximum profiles as described in the text) compared with GCM output (~80°N and L_s=150°–170°) and observational data (~60°–90°S and L_s=300°–360°) . Note the vertical scale changes from one row to the next. (a) profiles compared with zonal winds estimated from Cassini CIRS data (Achterberg et al., 2011) (b) with the zonal wind profile measured by Doppler tracking of the Huygens probe, multiplied by 0.3 to take into account the latitude (c) zonal winds from the TitanWRF GCM—profiles from several Titan days and local times are shown, the two sets of curves corresponding to 77°N (solid) and 82°N (dashed). The variation with latitude here is rather strong, and much larger than the diurnal or day–day variations. The 77°N case drives the formulation of our maximum envelope (d) zonal winds from the Köln GCM are rather small (e) and (f) zonal winds from the UCLA and IPSL GCMs are both somewhat higher than the Köln model (g) and (h) as (b) and (c) but zoomed in to the troposphere (i) Cassini cloud-tracking data as described in Fig. 2 (ellipses) are used to set the nominal profile. (a) Cassini CIRS, (b) Huygens DWE=0.3, (c) TitanWRF GCM, (d) Koni GCM, (e) UCLA GCM, (f) LMD/IPSL GCM, (g) Huygens DWE=0.3, (h) TitanWRF GCM and (i) Cassini ISS/VIMS.

3.2. Global circulation models

Since the first efforts by Del Genio et al. (1993)[1] and Hourdin et al. (1995), the number and fidelity of numerical models of Titan's global winds have both progressively increased. Here we present results from four modern models. The present paper is not intended as a model intercomparison or evaluation exercise, but rather (in the spirit of ensemble climate forecasting) to assess the likely envelope of winds for the specific location and season of interest, while avoiding reliance on the specific assumptions embedded in a single model.

As discussed in Friedson et al. (2009), a key discriminator in Titan GCMs appears to be the extent to which they predict the zonal superrotation. The earliest Titan-specific GCM, the LMD (Hourdin et al., 1995) model, made reasonably accurate estimates of the Huygens descent zonal winds, obtaining slightly less than the observed magnitude and gradient, including the inflection at 60–80 km. A 2D version of this model (Rannou et al., 2004), in which the 3D effects (eddy transport of angular momentum) required to produce superrotation were parameterized based on the original 3D model, and in which radiatively active haze was coupled to the dynamics via advection, improved the match, and the output from this model was encapsulated in a database (Rannou et al., 2005). However, both the LMD and Flasar models overpredicted tropospheric zonal winds. More typically, GCMs have tended to greatly underpredict the stratospheric superrotation, although some of the latest models show better success in this respect, and one (TitanWRF, Newman et al., 2011) predicts superrotation magnitudes similar to those observed.

The four models under consideration are mentioned briefly below.

[1] Actually just a slowly-rotating Earth model, rather than a Titan model per se.

Table 2
Model wind profile and relevant descent parameters at representative heights. Atmospheric density is from the nominal Yelle model. Note that the nominal meridional speed *V*nom is zero throughout—the minimum and maximum are given by $\pm|V|_{max}$.

Altitude (km)	Density (kg/m^3)	Gravity (m/s^2)	U_{min} (m/s)	$U_{nominal}$ (m/s)	U_{max} (m/s)	$\|V\|_{max}$ (m/s)
170	0.0030	1.19	−3.0	22.0	50.0	3.3
150	0.0051	1.21	−3.0	22.0	50.0	3.1
130	0.0088	1.22	−3.0	22.0	50.0	3.0
110	0.02	1.24	−3.0	22.0	49.9	2.8
90	0.03	1.26	−3.0	22.0	49.6	2.6
80	0.05	1.27	−3.0	21.9	48.9	2.5
70	0.08	1.28	−3.0	21.7	47.4	2.4
60	0.18	1.29	−3.0	21.1	44.0	2.3
50	0.36	1.30	−3.0	19.1	37.4	2.2
44	0.52	1.31	−3.0	16.6	31.7	2.1
38	0.76	1.31	−3.0	13.0	25.0	2.1
32	1.1	1.32	−3.0	9.0	18.3	2.0
26	1.55	1.32	−3.0	5.4	12.6	1.9
20	2.16	1.33	−3.0	2.9	8.1	1.8
18	2.4	1.33	−3.0	2.3	7.0	1.7
16	2.65	1.33	−3.0	1.9	6.0	1.7
14	2.93	1.34	−3.0	1.5	5.1	1.6
12	3.24	1.34	−3.0	1.2	4.3	1.6
10	3.56	1.34	−3.0	0.9	3.6	1.5
8	3.91	1.34	−3.0	0.7	3.1	1.5
6	4.27	1.34	−3.0	0.6	2.6	1.4
5	4.46	1.34	−3.0	0.5	2.4	1.4
4	4.67	1.35	−2.9	0.4	2.2	1.3
3	4.86	1.35	−2.9	0.4	2.0	1.3
2	5.05	1.35	−2.6	0.3	1.8	1.2
1	5.24	1.35	−2.2	0.3	1.7	1.2

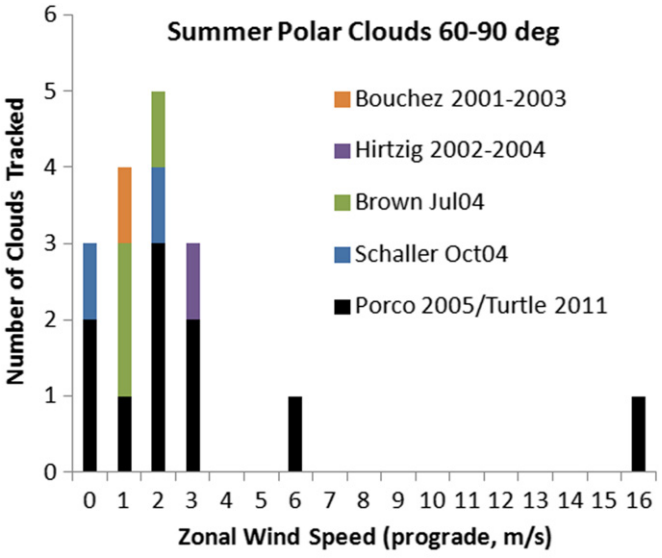

Fig. 2. Histogram of summer polar wind speeds derived from cloud-tracking by various authors as described in the text. Apart from one outlier, interpreted to be at higher altitudes, the data strongly cluster around 2 m/s prograde.

3.2.1. *TitanWRF*

The TitanWRF model (Richardson et al., 2007; Newman et al., 2011) extends from the surface to ~400 km altitude, and has been shown to generate low-latitude superrotation close to that observed, albeit peaking at slightly lower altitudes (most likely due to the proximity of the model top and/or the lack of haze advection in this version of the model). Newman et al. (2011) found the production of eddies that are key to the generation of superrotation to be highly sensitve to the amount of dissipation in the model dynamics, and to be prevented when horizontal diffusion within the model (included to parameterize sub-grid scale mixing processes) is too large. They obtained most realistic results when little or no explicit horizontal diffusion of angular momentum or temperature was included (though, as with most grid point models, TitanWRF also contains a small amount of implicit diffusion in its solver). The results shown here come from a 'dry' version of TitanWRF (i.e., with no methane cycle or associated latent heating effects are included) and the simulation was performed assuming a flat, homogeneous surface with no lakes but including the diurnal cycle of solar forcing and the impact of gravitational tides.

3.2.2. *Köln–Tokano*

The Köln GCM (Tokano et al., 1999) has been refined to include local surface properties associated with the seas. The effects of the seas, and of different compositions thereof, were explored in Tokano (2009), as well as Lorenz et al. (2012): in particular, it was found that a methane-rich composition sees rather little diurnal change in temperature and somewhat weaker winds, compared with the model with an ethane-rich sea composition. This presumably reflects that latent heat of methane evaporation in the former case 'soaks up' any excess solar flux in the surface energy balance, whereas less volatile ethane can warm up and drive 'sea breeze' circulation. The results reported here all assume the ethane-rich surface model.

3.2.3. *UCLA-Mitchell*

The third model considered is an idealized GCM used in climate studies by Mitchell et al. (2008). This model has a simplified radiative scheme and in fact uses longitudinally-symmetric solar forcing (i.e., there is no diurnal forcing). One distinction of this model over the others, though, is the inclusion of a moist convection scheme. Despite the lack of diurnal forcing, interesting longitudinal variability emerges due to the propagation of atmospheric waves (e.g., Mitchell et al. 2011).

3.2.4. *IPSL-Charnay*

The fourth model considered is a new refinement of the LMD (IPSL) model (Lebonnois et al., 2012; Charnay et al. 2012). A notable feature is the inclusion of an explicit boundary layer scheme, and indeed the interaction of the Hadley circulation with the planetary boundary layer (PBL) appears to successfully predict the near-surface atmospheric structure as measured by the Huygens probe.

3.3. *Zonal wind summary*

Reviewing Fig. 1, we see that the Cassini observations essentially describe 3 points (10–20 km, ~45 km and >200 km), which anchor the model and more or less explicitly determine the choice of the two parameters used in our 'nominal' profile. The scaled Huygens profile has a more complex shape but is broadly consistent with our analytic curve.

It is seen that most of the GCMs predict rather low zonal wind speeds at this latitude. An exception is the TitanWRF model, and it is the results of this model that drive the maximum value of our specification. The other three GCMs indicate rather modest zonal winds, although not substantially at odds with observations in the troposphere.

In determining the landing footprint of a spacecraft, the horizontal displacement *D* of the landing point from the start of descent is the result of the convolution of the wind profile with the time spent at each altitude. In effect, the displacement is a weighted average of the wind profile. The weighting will depend on the speed as a function of altitude: for a single parachute

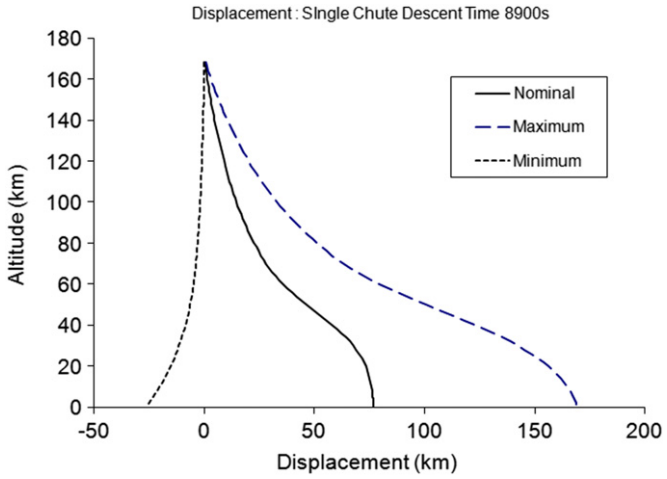

Fig. 3. Zonal wind drift ($dD/dz=u/(dz/dt)$) with altitude for the nominal, maximum and minimum wind (u) models as described in the text, assuming a parachute deployment at 170 km and a constant ballistic coefficient (mass divided by parachute drag area) sized to match the total descent time of the Huygens probe. Most of the displacement occurs over the altitude range 80–30 km : above this range the spacecraft falls too quickly (dz/dt) to be displaced far, and below 30 km the winds are weak.

design, this weighting function can be approximated by the inverse square root of atmospheric density at each altitude. This is because the vehicle can be assumed to be at terminal velocity, where weight balances drag. Since drag is proportional to density and the square of velocity and weight is roughly constant, the inverse root proportionality results (this is a slight approximation, since gravity and hence weight is a function of altitude (see Table 2), and parachute and vehicle drag coefficients may be functions of Mach and Reynolds numbers which change with altitude).

Fig. 3 plots the displacement as a function of altitude for the present wind model and a single parachute sized to give a total descent time equal to that of the Huygens probe. A heavier vehicle, or one with a smaller parachute, would fall faster and thus be displaced less; conversely, a vehicle that (as Huygens) spent time under a larger parachute at high altitude would be displaced more. 50% of the displacement in the example shown takes place between 30 and 80 km, whereas for Huygens 50% occurred above 100 km.

4. Meridional winds

The zonally-symmetric haze structure of Titan immediately suggests that meridional motions in the stratosphere are modest, and for Huygens mission planning (and indeed for the recovery of the zonal winds from Doppler measurements) the meridional winds were assumed to be zero. Cloud-tracking observations by Cassini yielding zonal and vertical winds (Porco et al., 2005 and Griffith et al., 2005—see previous section) do not indicate any meridional motion. Assuming that meridional motions could be measured with the same precision as zonal winds, an upper limit of 1–2 m/s is indicated.

Thus one of the surprises of the Huygens descent was its nonzero meridional motion. Karkoschka et al. (2007) used descent imaging from the Huygens probe to determine that the probe drifted south by 1 km between the altitudes of 40 km and 20 km (an interval of ~2200 s), implying winds of ~0.5 m/s. The probe was drifting in a SSE direction just prior to landing at ~0.3 m/s.

Pogrebenko et al. (2009) report an analysis of the tracking of the Huygens probe using an elaborate VLBI (Very Long Baseline Interferometry) experiment, which suggests a meridional drift of perhaps 20 km over the 500–5500 s period of probe descent, thus an averaged meridional motion of $\sim 3.5 +/- 0.4$ m/s between 120 km and 20 km. This result has only been documented in detail in an unrefereed ESA contract report (Pogrebenko et al., 2009), and thus must be considered somewhat less certain than the DISR result above (with which it somewhat disagrees)., In the interests of defining a conservative (inclusive) wind envelope we have nonetheless taken it into account here.

There are likely four principal contributions (all likely less at high latitudes than at the Huygens site) to these meridional motions. The first is the mean overturning circulation. The mean stratospheric meridional winds are certain to be considerably weaker than their zonal counterparts, as evidenced by the persistent and pronounced longitudinal symmetry in Titan's haze, temperatures and composition. On the large scale, the Hadley circulation transports some amount of the haze from the summer to the winter hemisphere. This requires $v > \sim 1$ cm/s at the ~200 km altitude of the top of the main haze layer. Rannou et al. (2002) show that the detached haze layer may be associated with meridional winds of ~2.5 m/s at 450 km. Interpretation of Voyager thermal infrared spectra (Flasar et al., 1981) for the stratosphere suggest $v \sim 1$ mm/s. However, these results reflect long-term zonal mean transports; it is possible that these transports are effected by variable winds (eddies), that are locally rather stronger than this. Further, while a single pole-pole cell is the canonical description of the circulation, there may be separate counterrotating cells at low altitude and/or very high latitude. Without knowing the potential boundary of such a cell, it is difficult to consider the direction of the meridional component to be deterministic at high latitudes. If the low-latitude VLBI result indicated above is correct, it is more likely to have been influenced at high altitude by the mean overturning circulation, which must be lower in magnitude at the high latitudes of interest to this paper. We accordingly scale the value down by a factor of 3, as for the Huygens zonal wind results. The DISR result at lower altitude may be influenced by a wider range of factors, listed below, which may not decline at high latitude to the same extent, so we consider this value as is, without a latitude correction.

The second contribution is that due to the gravitational tide in the atmosphere (Lorenz, 1992). This causes a diurnally-repeating cycle of tidal accelerations which Tokano and Neubauer (2002) predicted with their GCM to cause winds with a meridional component of ~0.5 m/s near surface at the equator, and less at higher altitudes and latitudes.

Perhaps the most significant deterministic contribution may be due to the offset of the center of the superrotating wind field from Titan's geometric pole as first noticed in thermal IR data (Achterberg et al., 2008) and subsequently confirmed in near-IR imaging (Roman et al., 2009). Specifically, the field is displaced by 4°, and thus (depending on the azimuth) may introduce a component of $\sin(4^\circ) \sim 0.07$ of the rotating wind field in the meridional direction. The tilt angle may vary with season, but at $L_s = 160^\circ - 170^\circ$ it is predicted to be almost the same as seen by Cassini (Tokano, 2010). However, since the zonal wind is weak near the summer pole the meridional wind should also be weaker than near the winter pole.

An additional factor may be 'sea breeze' circulation driven by the contrasts in albedo, thermal inertia, or evaporation between land and sea surfaces. These effects are pointed to in global modeling by Tokano (2009), but should be explored in more detail in mesoscale models. In principle such circulation may be deterministic as a function of location and time of day.

A fifth component, which is essentially a stochastic contribution, is the possibility of inflow or outflow related to a methane rainstorm. Such features should occur (Lorenz and Turtle, 2012) at a given location during polar summer for only 10–100 h out of

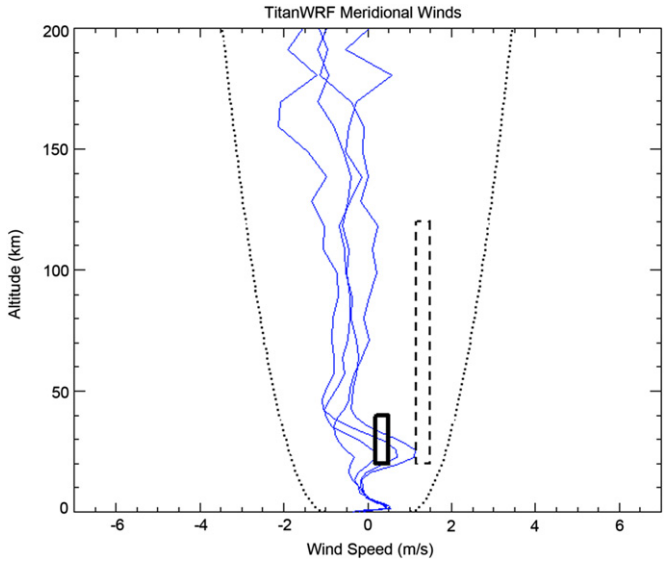

Fig. 4. Meridional Wind speed model and relevant data. The nominal model is for zero wind speed throughout: the dotted parabolic lines show the max/min model envelope. The solid 'curves are meridional velocities at several instants at 77°N and 82°N from the TitanWRF GCM for L_s=160°. The solid box shows the Huygens DISR observation of drift near the surface (uncorrected for latitude). The dashed box shows the Huygens drift estimated from VLBI, divided by 3 to account for latitude.

the ~50,000 year season, or <0.2% of the time and can therefore be neglected for the present study.

Wave activity in the atmosphere is likely to be a significant contributor to meridional motions, but there is little observational data to constrain this (indeed, the meteorological record from a fixed or even slowly-drifting lander will be one of the best ways to detect such waves). Wave activity is seen in GCMs, although here we simply report the total meridional speeds, without decomposing into waves, tides etc. TitanWRF simulations suggest meridional speeds at 70°N for the relevant season of ~0.3–0.4 m/s. Friedson et al. (2009) predict near-surface meridional speeds of 0.1–0.2 m/s. Rather stronger meridional motions are predicted by Tokano (2007) who indicates that the meridional component of wind can be ~0–1 m/s throughout the column.

The meridional wind model and constraints are summarized in Fig. 4. The nominal meridional wind is assumed to be zero. A symmetric specification is proposed for the 99% envelope, that increases modestly with altitude, specifically $|v| < 1+3(z/300)^{0.5}$, where v is in m/s and z in km. The specification conservatively spans the values of the raw DISR tracking and the corrected VLBI as well as all GCM values.

5. Vertical winds

The Huygens probe (Mäkinen et al., 2006) measured vertical winds in the troposphere with a mean value of 0.05 m/s upwards. Some subsidence was measured in the stratosphere, averaging around 0.1 m/s with a peak of 0.5 m/s, possibly related to a gravity wave.

Overall, the summer hemisphere of Titan sees upwelling in the stratosphere due to the thermally-direct mean overturning circulation. For mission design purposes, however, vertical winds can likely be neglected in that these expected values are so small, although if descent time or speed are critical, it might be prudent to assume a zero mean vertical wind with a standard deviation of ~0.1 m/s. It should be noted, however, that a small (<0.5%) probability of encountering convective updrafts with speeds of 1–10 m/s exists, as was noted for Huygens.

6. Surface winds

The caveat was noted in "Zonal wind data" section that the profile specification should not be applied below ~2 km. In general applying the profiles down to the surface will not be problematic (e.g., for generating landing point dispersions in Monte Carlo studies). However, these simple expressions do not capture the drop in wind speed near the surface, and so will overestimate the horizontal velocity of a descending vehicle. Since this may be a crucial consideration, we discuss surface wind speed distributions explicitly here.

In many terrestrial applications where there is information on surface roughness and on convective stability, a logarithmic wind profile is used. However, when such information is not well-constrained, as is usually the case for offshore engineering problems, a convenient and reasonably accurate approach is to assume a power law (Hsu et al., 1994). This takes the form $U(z)=U_{ref}\ (z/z_{ref})^{\alpha}$, where z is the height of interest and U_{ref} is the speed at a reference height z_{ref}, with α=0.11 for the open sea, which is appropriate for the present application (α~0.14 is more typical for land surfaces).

In fact some results previously reported as 'surface winds' (Lorenz et al., 2010, 2012) were in fact simply winds in the lowest model cell of the relevant GCM (for TitanWRF in the case of Lorenz et al. (2010, 2012), this corresponded to an altitude of ~90 m; for the Köln GCM in Lorenz et al. (2012) it was 300 m). Applying the power law correction given above suggests that the wind at anemometer height U_{10} (a height of 10 m is used widely in air:sea interaction studies) should be a factor of 0.68 lower for the Köln model, a factor of 0.78 for TitanWRF, and a factor of 0.65 for the UCLA model for which the lowest model layer corresponds to 500 m. Some support for the decline in winds near the surface is evident in Huygens data. The average of the Huygens Doppler wind measurements (specifically, the estimated zonal wind component, as listed in the ZONALWIND.TAB dataset as archived

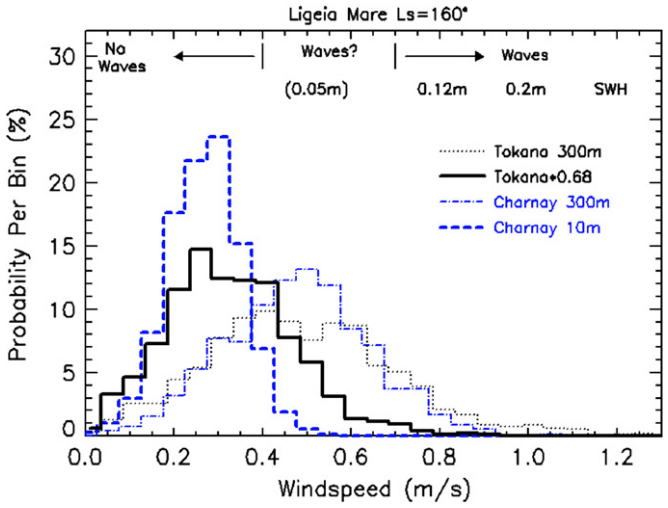

Fig. 5. Histograms of surface and near-surface wind speeds showing boundary layer correction. The dotted line is winds at 300 m from the Köln GCM by Tokano: this is scaled by 0.68 in order to estimate the winds at 10 m anemometer height to yield the solid curve. Winds at 300 m from the Charnay IPSL GCM are shown as a dash-dot line, whereas 10 m winds from the same model are shown as a dashed line. The two models agree closely at 300 m, and the power-law correction to the Köln 300 m value to 10 m brings it into reassuringly good agreement with the IPSL 10 m value. In the upper part of the plot, the threshold wind speeds for generating waves (Hayes et al., submitted) are noted.

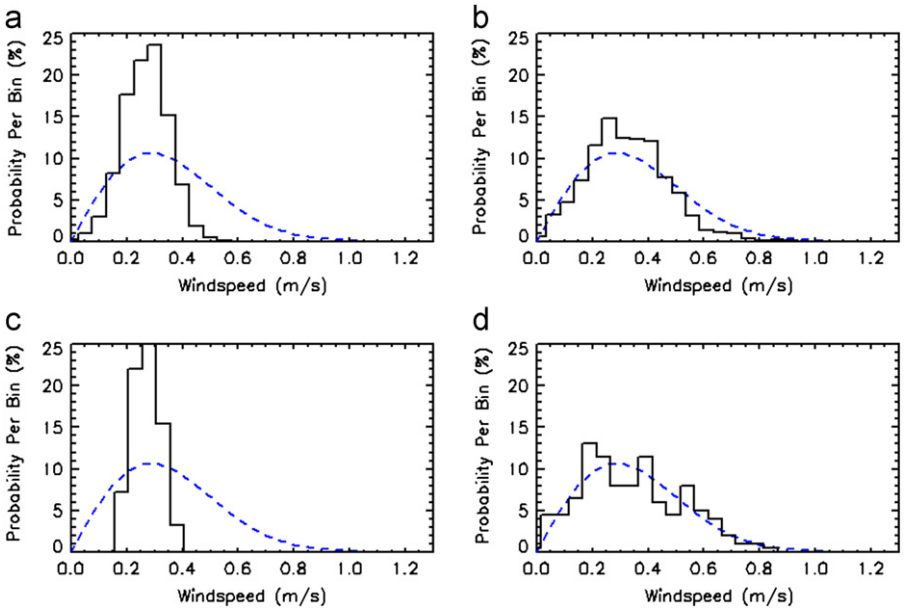

Fig. 6. Surface (10 m height) speed distributions for the four GCMs (solid line histograms) described in the text, calculated from data over the interval $L_s=150^\circ$ to $L_s=170^\circ$. It is evident that the most likely wind speed is about 0.3 m/s, and that winds do not exceed 0.9 m/s. A Weibull distribution with $C=0.4$ m/s and shape parameter $k=2$ is shown (smooth dashed line) for comparison, with these values chosen so that probabilities for the fastest winds are slightly higher than all GCMs and thus serves as a conservative description. (a) Chamay IPSL, (b) Takana Kain U300=0.68, (c) Mitchell UCLA U500=0.65 and (d) Newman TitanWRF U90=0.78.

on the Planetary Data System Atmospheres Node) in the lowest 500 m of the atmosphere at the Huygens landing site is ~0.45 m/s – see also Fig. 7 in Folkner et al. (2006) – and the average in the lowest 250 m of descent is 0.28 m/s. The winds in the lowest 30 m of the atmosphere were also estimated by observing the drift of the parachute at ~0.3 m/s (Karkoschka et al., 2007) and the cool-down of the probe after landing indicated winds at the ~0.5 m level of less than 0.2 m/s (Lorenz, 2006).

The IPSL GCM has an explicit boundary layer model (albeit assuming uniform surface thermal and roughness properties). Wind speeds at a 300 m level and at 10 m have been extracted. It can be seen in Fig. 5 that the Köln GCM and IPSL models at 300 m have rather similar probability distributions, and scaling the Köln values by 0.68 brings them into good agreement with the IPSL wind speeds computed for 10 m. (Another approach would be to use surface friction velocity from the models to estimate winds at 10 m height—in essence all these methods are ultimately equivalent.) The values plotted are instantaneous wind speed extracted from the models 20 or 24 times per Titan day, over the period $L_s=150^\circ$–170^o.

Following practice in the wind energy industry and Lorenz (1996) and Lorenz et al. (2012), we use a Weibull distribution to analytically describe the probability of encountering a surface wind (U_{10}) of a given speed. Fig. 6 shows the Weibull description of the cumulative form $P(>U)=\exp(-[U/C]^k)$. The parameters have been chosen (scale speed $C=0.4$ m/s and shape parameter $k=2.0$) to span the strongest winds—those of the TitanWRF model. It is evident that the most probable surface winds are around 0.3 m/s, and that winds of 0.9 m/s or higher are unlikely to be encountered.

7. Conclusions and future work

We find that zonal winds near the summer pole will be rather weaker (by perhaps a factor of 3 or more) than those at low latitude, and we have defined a model profile of the expected wind speeds with altitude and the associated maximum and minimum values.

Meridional and vertical winds are everywhere rather weak, although winds at the sea surface can have a significant meridional component. The analytic expressions for the model are given in the text, and a set of specific values are listed in Table 2. The ranges given should be considered '99%' values. The Weibull distribution of surface winds in "Surface winds" section should similarly not be considered accurate beyond 99%, since local convection is not taken into account.

The correction of model output (wind speed in the lowest cell in the GCM grid) by a simple power-law altitude function has been investigated, and found to reproduce the results of an explicit boundary layer scheme rather well. Some previously-published speed estimates (Lorenz et al., 2010, 2012) are 20–30% too high to be applicable as U_{10}.

In order to yield a tighter estimate of where a descending capsule may land, it would be desirable to narrow the dispersions in the present model which is somewhat conservatively specified. We may expect ongoing Cassini data to provide progressively more observational constraints, at ever-more-relevant seasons. However, as discussed in "Wind modeling for planetary missions" section, in principle hundreds of independent observational data points falling close to our nominal specification would be needed to robustly tighten the envelope overall. On the other hand, since much of the displacement occurs in the 30–60 km altitude range, and the nominal model is forced by only a single (apparent) cloud track at of ~15 m/s, a handful of new data at this altitude could shift at least the nominal profile.

At present the envelope is forced to accommodate values from all Global Circulation Models, and specifically the maximum profile is driven by the values from the TitanWRF GCM (which also gives the strongest surface wind predictions). Various parameters in a GCM can be adjusted (notably the diffusion or damping terms invoked in part to avoid numerical instabilities) which may affect the results. An obvious avenue for GCM improvement is the introduction of estimated surface parameter fields from Cassini data, such as surface albedo, thermal inertia, and topography. Additionally, model treatment of many physical processes can also be improved, such as the specification of the radiative scheme (rather simple in some models) or the treatment

of moist convection. Since precipitation occurs only 0.02–0.2% of the time (Lorenz and Turtle, 2012), moist convective processes are not explicitly evaluated in the present paper, although mesoscale modeling (Barth and Rafkin, 2007) suggests their local effects on winds could be significant.

The current model is an instantaneous specification of windspeeds, for the descent and splashdown of a parachute-borne probe. There are other applications where the time series of vector winds on the surface is of interest, for example on predicting the drift trajectory of a floating capsule (e.g., Lorenz et al., 2012, though note that that work overpredicts surface winds due to the noninclusion of the boundary layer correction), or on the temporal decorrelation of meteorological variables (i.e., if it is a windy day on one day, will it be windy on the next?). An investigation of these statistical properties will be the subject of future work.

Acknowledgments

R. Lorenz was supported for this work by APL internalfunds, and by the NASA Discovery program (Titan Mare Explorer Phase A study). C. Newman acknowledges the support of the NASA Outer Planets Research Program and access to the NASA Ames High End Computing facility, on which all simulations were performed. We thank Mark Johnson and Bill Willcockson of Lockheed Martin Space Systems for discussions on the influence of descent winds on landing footprints. We thank F. M. Flasar and another (anonymous) reviewer for useful comments on the model and the paper.

References

Achterberg, R.K., Conrath, B.J., Gierasch, P.J., Flasar, F.M., Nixon, C.A., 2008. Observation of a tilt of Titan's middle-atmospheric superrotation. Icarus 197, 549–555.

Achterberg, R.K., Gierasch, P.J., Conrath, B.J., Flasar, F.M., Nixon, C.A., 2011. Temporal variations of Titan's middle-atmospheric temperatures from 2004 to 2009 observed by Cassini/CIRS. Icarus 211, 686–698.

Allison, M., 1992. A preliminary assessment of the Titan planetary boundary layer, pp.113–118 in Proceedings of the Symposium on Titan, ESA SP-338, B. Kaldeich (Ed.), European Space Agency, Noordwijk, 1992.

Barth, E. L. and S. C. R. Rafkin, TRAMS: a new Dynamic Cloud Model for Titan's Methane Clouds, Geophysical Research Letters, 34, L03203.

Bouchez, A., Brown, M., 2005. Statistics of Titan's South Polar Tropospheric Clouds. The Astrophysical Journal 618, L53–L56.

Brown, R.H., et al., 2006. Observations in the Saturn system during approach and orbital insertion, with Cassini's visual and infrared mapping spectrometer (VIMS). Astronomy and Astrophysics 446, 707–716.

Brown, R., Lebreton, J.-P., Waite, H. (Eds.), 2009. Springer, New York 600pp.

Bird, M.K., et al., 2005. The vertical profile of winds on Titan. Nature 438, 800–802.

Charnay, B., Lebonnois, S., 2012. Two boundary layers in Titan's lower troposphere inferred from a climate model. Nature Geoscience 2012 10.1038NGEO1374.

Coustenis, A., Taylor, F., 2008. Titan: Exploring an Earthlike World. World Scientific, Singapore 412pp.

Del Genio, A.D., Zhou, W., Eichler, T.P., 1993. Equatorial superrotation in a slowly rotating GCM: implications for Titan and Venus. Icarus 101, 1–17.

Flasar, F.M., Allison, M.D., Lunine, J.I., 1997. Titan zonal wind model. In: Wilson, A. (Ed.), Huygens: Science, Payload, and Mission. European Space Agency, Noordwijk, pp. 287–298, ESA SP-1177.

Flasar, F.M., et al., 2005. Titan's atmospheric temperatures, winds, and composition. Science 308, 975–978.

Flasar, F.M., Baines, K.H., Bird, M.K., Tokano, T., West, R.A., 2010. Atmospheric dynamics and meteorology, In: Brown, R.H., Lebreton, J.-P., Waite, J.H. (Eds.) Titan from Cassini-Huygens. Springer. pp. 323–352.

Flasar, F.M., Samuelson, R.E., Conrath, B.J., 1981. Titan's atmosphere: temperature and dynamics. Nature 292 (5825), 693–698.

Folkner, W.M., et al., 2006. Winds on Titan from ground-based tracking of the Huygens probe. Journal of Geophysical Research 111, E07S02.

Friedson, A.J., West, R.A., Wilson, E.H., Oyafuso, F., Orton, G.S., 2009. A global climate model of Titan's atmosphere and surface. Planetary and Space Science 57, 1931–1949.

Griffith, C.A., Penteado, P., Baines, K, Drossart, P, Barnes, J, Bellucci, G, Bibring, J, Brown, R, Buratti, B, Capaccioni, F, Cerroni, P, Clark, R, Combes, M, Coradini, A, Cruikshank, D, Formisano, V, Jaumann, R, Langevin, Y, Matson, D, McCord, T, Mennella, V, Nelson, R, Nicholson, P, Sicardy, B, Sotin, C, Soderblom, LA, Kursinski, R., 2005. The evolution of Titan's mid-latitude clouds. Science 310, 474–477.

Hayes, A.G., Lorenz, R.D., Donelan, M.A., Schneider, T., Lamb, M.P., Fischer, W.W., Mitchell, J.M., Schlichting, H.E., Manga, M., Lunine, J.I., Graves, S.D., Tolman, H.L., Aharonson, O., Encrenaz, P., Ventura, B., Casarano, D., the Cassini RADAR Team. Wind Driven Capillary-Gravity Waves on Titan's Lakes: Hard to Detect or Non-Existent? Icarus, submitted for publication.

Hirtzig, M., Coustenis, A., Gendron, E., Drossart, P., Negrão, A., Combes, M., Lai, O., Rannou, P., Lebonnois, S., Luz, D., 2006. Monitoring atmospheric phenomena on Titan. Astronomy and Astrophysics 456, 761–774.

Hourdin, F., Talagrand, O., Sadourny, R., Régis, C., Gautier, D., McKay, C., 1995. General circulation of the atmosphere of Titan. Icarus 117, 358–374.

Hsu, S.A., Meindl, E.A., Gilhousen, D.B., 1994. Determining the Power-Law Wind-Profile Exponent under Near-Neutral Stability Conditions at Sea. Journal of Applied Meteorology 33, 757–772.

Hubbard, W.B., et al., 1993. The 28 Sag occultation of Titan. Astronomy and Astrophysics 269, 541–563.

Justus, C. G., Duvall, A., & Keller, V. W., 2004. Engineering-level model atmospheres for Titan and Mars, pp. 311–316 in Wilson, A. (Ed.), Proceedings of the International Workshop Planetary Probe Atmospheric Entry and Descent Trajectory Analysis and Science, 6–9 October 2003, Lisbon, Portugal. ESA SP-544, pub. ESA, Noordwijk, Netherlands, 2004.

Karkoschka, E., Tomasko, M.G., Doose, L.R., See, C., McFarlane, E.A., Schröder, S.E., Rizk, B., Nov. 2007. DISR Imaging and the Geometry of the Descent of the Huygens Probe within Titan's Atmosphere. Planetary and Space Science 55, 1896–1935.

Kass, D.,J.T., Schofield, T., Michaels, S.C.R., Rafkin, M.I., Richardson, Toigo, A.D., 2003. Analysis of atmospheric mesoscale models for entry, descent, and landing. Journal of Geophysical Research 108, 8090.

Kostiuk, T., Fast, K.E., Livengood, T.A., Hewagama, T., Goldstein, J.J, Espenak, F., Buhl, D., 2001. Direct measurement of winds on Titan. Geophysical Research Letters 28, 2361–2364.

Kostiuk, T., Livengood, T.A., Sonnabend, G., Fast, K.E., Hewagama, T., Murakawa, K., Tokunaga, A.T., Annen, J., Buhl, D., Schmülling, F., Luz, D., Witasse, O., 2006. Stratospheric global winds on Titan at the time of Huygens' descent. Journal of Geophysical Research 111E07S03.

Lebonnois, S., Burgalat, J., Rannou, P., Charnay, B., 2012. Titan global climate model: a new 3-dimensional version of the IPSL Titan GCM. Icarus 218, 707–722.

Lorenz, R.D., 1992. Gravitational tide in the atmosphere of Titan. In Proceedings Symposium on Titan, Toulouse, ESA SP-338 (B. Kaldeich, Ed.), pp. 119–123. European Space Agency, Noordwijk, The Netherlands.

Lorenz, R.D., 1996. Martian Surface Windspeeds, described by the Weibull distribution. Journal of Spacecraft and Rockets 33, 754–756.

Lorenz, R.D., 2006. Thermal interaction of the Huygens probe with the Titan environment : surface wind speed constraint. Icarus 182, 559–566.

Lorenz, R.D., Mitton, J., 2008. Titan Unveiled. Princeton University Press. Princeton N.J.. 296 pp.

Lorenz, R.D., Newman, C., Lunine, J.I., 2010. Threshold of wave generation on Titan's lakes and seas: effect of viscosity and implications for Cassini observations. Icarus 207, 932–937.

Lorenz, R.D., Tokano, T., Newman, C.E., 2012. Winds and Tides of Ligeia Mare : application to the Drift of the Titan Mare Explorer (TiME) mission. Planetary and Space Science 60, 72–85.

Lorenz, R. D. and E. P. Turtle, 2012. How often does it Rain on Titan?, Abstract 2472, 42nd Lunar and Planetary Science Conference, Houston, TX, March 2012.

Mäkinen, J.T., Harri, A.-M., Tokano, T., Savijarävi, H., Siili, T., Ferri, F., 2006. Vertical atmospheric flow on Titan as measured by the HASI instrument on board the Huygens probe. Geophysical Research Letters 33, L21803.

Mitchell, J.L., 2008. The drying of Titan's dunes: Titan's methane hydrology and its impact on atmospheric circulation. Journal of Geophysical Research (Planets) 113, E12. http://dx.doi.org/10.1029/2007JE003017.

Mitchell, J.L., Ádámkovics, M., Caballero, R., Turtle, E., 2011. Locally enhanced precipitation organized by planetary-scale waves on Titan. Nature Geoscience 4, 589–592.

Newman, C.E., Lee, C., Lian, Y., Richardson, M.I., Toigo, A.D., 2011. Stratospheric superrotation in the TitanWRF model. Icarus 213, 636–654.

Pankine, A.A., Aaron, K.M., Heun, M.K., Nock, K.T., Schlaifer, S.R., Wyszkowsky, C.J., Ingersoll, A.P., Lorenz, R.D., 2004. Directed Aerial Robot Explorers (DARE) for Planetary Exploration. Advances in Space Research 33, 1825–1830.

Pogrebenko, S. V.; Gurvits, L. I.; Avruch, I. M.; Cimo, G. 2009. Huygens VLBI Trajectory—Evidence for Meridional Wind in Titan's upper Atmosphere, European Planetary Science Congress 2009, 14–18 September in Potsdam, Germany, p.199 (see also Report 'VLBI Observations of the Huygens Probe' ESA-ESTEC Contract No. 18386/NL/NR, JIVE Research Note #0011, Joint Institute for VLBI in Europe, P. . Box 2, 79900 AA Dwingeloo, The Netherlands, 15 October 2008).

Porco, C.C., et al., 2005. Imaging of Titan from the Cassini spacecraft. Nature 434, 159–168.

Rannou, P., Hourdin, F., McKay, C.P., 2002. A wind origin for Titan's haze structure. Nature 418, 853–856.

Rannou, P., Hourdin, F., McKay, C.P., Luz, D., 2004. A coupled dynamics-microphysics model of Titan's atmosphere. Icarus 170, 443–462.

Rannou, P., Lebonnois, S., Hourdin, F., Luz, D., 2005. Titan atmosphere database. Advances in Space Research 36, 2194–2198.

Richardson, M.I., Toigo, A.D., Newman, C.E., 2007. PlanetWRF: a general purpose, local to global numerical model for planetary atmospheric and climate dynamics. Journal of Geophysical Research 112, E09001.

Roman, M.T., West, R.A., Banfield, D.J., Gierasch, P.J., Achterberg, R.K., Nixon, C.A., Thomas, P.C., 2009. Determining a tilt in Titan's north–south albedo asymmetry from Cassini images. Icarus 203, 242–249.

Schaller, E., Brown, M., Roe, H., Bouchez, A., 2006. A large cloud outburst at Titan's south pole. Icarus 182, 224–229.

Sicardy, B., et al., 2006. The two Titan stellar occultations of 14 November 2003. Journal of Geophysical Research 111, E11S91 2006.

Tamppari, L.K., Barnes, J., Bonfiglio, E., Cantor, B., Friedson, A.J., Ghosh, A., Grover, M.R., Kass, D., Martin, T.Z., Mellon, M, Michaels, T., Murphy, J., Rafkin, S.C.R., Smith, M.D., Tsuyuki, G., Tyler, D., Wolff, M., 2008. Expected atmospheric environment for the Phoenix landing season and location. Journal of Geophysical Research 113E00A20.

Stofan, E.R., et al., 2007. The lakes of Titan. Nature 445, 61–64.

Tomasko, M.G., Archinal, B., Becker, T., Bezard, B., Bushroe, M., Combes, M., Cook, D., Coustenis, A., de Bergh, C., Dafoe, L.E., Doose, L., Douté, S., Eibl, A., Engel, S., Gliem, F., Grieger, B., Holso, K., Howington-Kraus, A., Karkoschka, E., Keller, H.U., Kirk, R., Kramm, R., Kuppers, M., Lellouch, E., Lemmon, M., Lunine, J., McFarlane, E., Moores, J., Prout, M., Rizk, B., Rosiek, M., Ruffer, P., Schroeder, S.E., Schmitt, B., See, C., Smith, P., Soderblom, L., Thomas, N., West, R., 2005. Rain, winds and haze during the Huygens probe's descent to Titan's surface. Nature 438, 765–778.

Tokano, T., Neubauer, F., 2002. Tidal winds on Titan caused by Saturn. Icarus 158, 499–515 2002.

Tokano, T., Lorenz, R.D., 2006. GCM Simulations of balloon trajectories on Titan. Planetary and Space Science 54, 685–694.

Tokano, T., Neubauer, F.M., Laube, M., McKay, C.P., 1999. Seasonal variation of Titan's atmospheric structure simulated by a general circulation model. Planetary and Space Science 47, 493–520.

Tokano, T., 2007. Near-surface winds at the Huygens site on Titan: interpretation by means of a general circulation model. Planetary and Space Science 55, 1990–2009.

Tokano, T., 2009. Impact of seas/lakes on polar meteorology of Titan: Simulation by a coupled GCM-Sea model. Icarus 204, 619–636.

Tokano, T., 2010. Westward rotation of the atmospheric angular momentum vector of Titan by thermal tides. Planetary and Space Science 58, 814–829.

Turtle, E.P., et al., 2009. Cassini Imaging of Titan's High-Latitude Lakes, Clouds, and South-Polar Surface Changes. Geophysical Research Letters 36, L02204 10.1029:2008GL036186.

Turtle, E.P., Del Genio, A.D., Barbara, J.M., Perry, J.E., Schaller, E.L., McEwen, A.S., West, R.A., Ray, T.L., 2011. Seasonal changes in Titan's meteorology. Geophysical Research Letters 38 (L03203), 2011.

Witasse, O., Lebreton, J-P., Bird, M.K., Dutta-Roy, R., Folkner, W.M., Preston, R.A., Asmar, S.W., Gurvits, L.I., Pogrebenko, S.V., Avruch, I.M., Campbell, R.M., Bignall, H.E., Garrett, M.A., van Langevelde, H.J., Parsley, S.M., Reynolds, C., Szomoru, A., Reynolds, J.E., Phillips, C.J., Sault, R.J., Tzioumis, A.K., Ghigo, F., Langston, G., Brisken, W., Romney, J.D., Mujunen, A., Ritakari, J., van't Klooster, C.G.M., Blancquaert, T., Coustenis, A, Gendron, Eric, Hirtzig, M., Negrao, A., Sicardy, B., Luz, D., Kostiuk, T., Livengood, T.A., Hartung, M., de Pater, I., Ádámkovics, M., Lorenz, R.D., Roe, H., Schaller, E., Brown, M., Bouchez, A.H., Trujillo, C.A., Buratti, B.J., Caillault, L., Magin, T., Bourdon, A., Laux, C., 2006. Overview of the coordinated ground-based observations of Titan during the Huygens mission. Journal of Geophysical Research - Planets 111, E07S01.

Yelle, R.V., Strobel, D.F., Lellouch, E., Gautier, D., 1997. Engineering models for Titan's atmosphere. In: Wilson, A. (Ed.), Huygens: Science, Payload, and Mission, 1997. European Space Agency, Noordwijk, pp. 243–256, ESA SP-1177.